Hindawi
Advances in Materials Science and Engineering
Volume 2019, Article ID 3732160, 13 pages
https://doi.org/10.1155/2019/3732160

Research Article

Optimization and Hydration Mechanism of Composite Cementing Material for Paste Filling in Coal Mines

Jinxiao Liu,[1,2,3,4] **Wenxin Li**,[1,3] **Feng Zhang**,[3] **Xinguo Zhang**,[1,3,4] **Lianjun Chen**,[1,3] **and Yongle Liu**[3]

[1]*Mine Disaster Prevention and Control-Ministry of State Key Laboratory Breeding Base, Shandong University of Science and Technology, 579 Qianwangang Rd, Huangdao District, Qingdao 266590, China*
[2]*Key Laboratory of Deep Coal Mine Excavation Response & Disaster Prevention and Control, Anhui University of Science and Technology, Huainan 232001, China*
[3]*College of Mining and Safety Engineering, Shandong University of Science and Technology, 579 Qianwangang Rd, Huangdao District, Qingdao 266590, China*
[4]*State Key Laboratory of Mining Disaster Prevention and Control Co-founded by Shandong Province and the Ministry of Science and Technology, National Engineering Laboratory for Backfill Coal Mining, Shandong University of Science and Technology, Qingdao 266590, China*

Correspondence should be addressed to Jinxiao Liu; liujinxiao1999@126.com and Wenxin Li; li17753299337@163.com

Received 23 June 2019; Revised 23 July 2019; Accepted 26 October 2019; Published 7 December 2019

Academic Editor: Frederic Dumur

The low early strength of materials for paste filling in mines caused by low early strength of composite cementing material has been a severe issue. In this study, the effects of sulphoaluminate cement and gypsum on strengths of composite cementing material were investigated experimentally by employing the constrained formulation uniform design. With the content of the sulphoaluminate cement below 14% and the content of the gypsum below 16%, the compressive strengths of composite cementing materials increased, especially early strength. However, the initial and final setting time does not meet the engineering requirements in this case. Optimization tests of composite additives demonstrated that H_2BO_3(0.3%) + Na_2SO_4(0.1%) and H_2BO_3(0.3%) + $NaNO_2$(0.1%) were ideal setting retarding and early strengthening composite additives as they can both reduce the initial and final setting time and enhance compressive strengths of composite cementing material. Investigations by XRD and SEM revealed that the hydration products of composite cementing material were dominated by AFt (ettringite) at the early stage and by C-S-H (hydrated calcium silicate) gel + CH (calcium hydroxide) gel at the middle and late stages. The hydration products of ratio-optimized composite cementing material do not restrain each other due to the generation sequence. Instead, they grew interactively and were coupled, thus facilitating the growth of the hardened body. This study can provide references for optimization of composite cementing material for paste filling in coal mines.

1. Introduction

In cementing filling, cementing agents (e.g., cement, red mud, and gypsum) were added into the filling materials, which were pumped to the underground to generate fillers with moderate strengths. The cement filler does not collapse even after partial or full relievation of its limiting conditions, thus supporting surrounding rocks and pillars. Hence, cementing filling technologies in mining can effectively extract limited resources and relieve its environment damages [1–3].

Cementing filling technologies have been widely employed since 1960s. For instance, pillars were extracted in the Mount Isa Mine in Australia using tailing cementing filling techniques, and the cement content was 12%. In 1980s and 1990s, new processes such as high-concentration filling, paste filling, waste stone cementing filling, and full tailing cementing filling have been developed and applied in various mines, including the Kidd Creek Mine, the Golden Giant Mine and the Louvicourt Mine in Canada, the Köln Mine in Germany, and the Cannington Mine in Australia [4–6].

In China, the development of cementing filling technologies can be divided into three stages. At the first stage (1960s), graded tailings were used as aggregates in cementing filling technologies. In 1968, cementing filling (in the Fankou lead-zinc mine) by graded tailings and cement was reported for the first time. At the second stage (1980s), full tailing and high-concentration cementing filling [7–12], high water rapid setting and full tailing cementing filling [13–15], and block stone cementing filling [16–21] dominated. At the third stage (1990s), paste and paste-like pumping cementing filling technology was developed [22–28].

Previous studies demonstrated that the properties of cementing material are key factors affecting its parameters such as filler strength and setting time [29–67]. As the requirement on early strength of fillers by paste filling in metal mining is not high, the cost-effective and readily accessible Portland cement can be used as the paste of cementing material. However, unlike paste filling in metal mining, the mining and filling processes of longwall workface in coal mines are strictly alternative (each for 8–10 h). Hence, paste filling in coal mining requires relatively high early strength. Owing to its long setting time and slow growth of early strength, the early performance of Portland cement must be enhanced before being used as dominant cementing fillers in paste filling.

Based on the practical requirements on performances (e.g., compressive strength and setting time) of filling paste cementing material for coal mining, Portland cement was used as the dominant material, with sulphoaluminate cement and gypsum as additives to enhance its early strength. The initial and final setting time of composite cementing material was controlled in 2.5~4 h and 3~4 h, respectively. First, ratios of Portland cement, sulphoaluminate cement, and gypsum in composite cementing material were optimized experimentally; then, additives were used to modify the composites. Finally, the hydration process was identified by investigating the hydration mechanism of composite cementing material to obtain that it meets the requirements of paste filling in coal mines.

2. Materials, Equipment, and Methods

2.1. Composition and Optimization Scheme of Composite Cementing Material. In this study, Portland cement was used as the main ingredient for paste cementing material, with sulphoaluminate and gypsum as supplemental ingredients to enhance the early strength of composite cementing material. The formulation of composite cementing material was determined by constrained formulation uniform design, and then the mechanical performances of the proposed composites were tested. Specifically, compressive strengths and the setting time of composite cementing materials with different ratios (D01~D15) at different ages were measured.

2.1.1. Raw Materials. The No. 42.5 Portland cement (chemical and mineral compositions are shown in Table 1) was purchased from Shandong Sunnsy Cement Group, the No. 42.5 rapid hardening sulphoaluminate cement (mineral composition is shown in Table 2) was from Shandong Jinyu Cement Co., Ltd., and the hardened gypsum (chemical composition is shown in Table 3) from Shandong Taihe Dongxin Group was calcinated.

2.1.2. Instruments. Table 4 summarizes the testing instruments.

2.1.3. Testing of Performances. In this study, the composite cementing materials consist of Portland cement, sulphoaluminate cement, and gypsum in different ratios. With guaranteed early strength of composite cementing material, the content of sulphoaluminate cement shall be minimized to reduce the cost. With reference of the results from other researchers, the optimized contents of sulphoaluminate cement, gypsum, and Portland cement were determined to be 0~20%, 0~20%, and 60%~100%, respectively. The constraints of corresponding formulation tests are as follows:

$$\begin{cases} X_1 + X_2 + X_3 = 1, \\ 0.6 \le X_1 \le 1, \\ 0 \le X_2 \le 0.2, \\ 0 \le X_3 \le 0.2. \end{cases} \quad (1)$$

Then, the corresponding testing scheme (15 sample groups, see Table 5) was developed using the constrained formulation design in the Uniform Design Version 3.0. The uniform design table used was $U_{31}^{*}(31^{10})$ with $D = 0.0908$ (see Appendix).

The raw materials were mixed and stirred to generate $70.7 \times 70.7 \times 70.7\ \text{mm}^3$ stock samples (Figure 1), which were cured at a relative humidity of 90% and a temperature of $20 \pm 2^{\circ}\text{C}$ to designated ages to obtain testing samples. According to the GB177-85 cement mortar strength testing method, the compressive strengths of samples at different ages were measured using the MTS-815 mechanical tester. In addition, the GB1346-89 cement standard consistency water consumption, setting time, and stability testing method were adopted to measure the setting time. The initial setting time is defined as the period from the start to the moment when slurry loses flow ability, during which the plasticity of cementing material paste remained constant. After initial setting, the cementing material paste was further hardened until its complete loss of plasticity, which corresponds to the final setting.

2.2. Modification Scheme of Optimized Composite Cementing Material. According to the results of mechanical performance tests, optimized formulations of composite cementing material with adequate early compressive strength were identified. The setting time was selected as the performance indicator of composite cementing material. The hydration of sulphoaluminate cement was initiated after 10 min and considerable quantity of gel was generated, resulting in too short setting time of composite cementing material. Therefore, the setting time shall be adjusted using composite additives such as setting retarding agents (e.g.,

Table 1: Chemical and mineral compositions of portland cement.

Material	Chemical constituents (%)					Mineral compositions (%)			
	SiO_2	Al_2O_3	Fe_2O_3	CaO	SO_3	C_3S	C_2S	C_3A	C_4AF
Portland cement	21.38	4.23	3.58	66.49	0.1	59.95	12.02	5.94	13.53

Table 2: Chemical and mineral compositions of sulphoaluminate cement.

Material	Chemical constituents (%)					Mineral compositions (%)			
	SiO_2	Al_2O_3	Fe_2O_3	CaO	SO_3	$C_4A_3\overline{S}$	β-C_2S	C_2F	f-SO_3
Sulphoaluminate cement	11.85	29.64	2.68	43.22	6.94	57.37	25.55	6.56	1.92

Table 3: Chemical composition of hardened gypsum.

Material	Chemical constituents (%)							
	CaO	Al_2O_3	Fe_2O_3	SO_3	SiO_2	MgO	Na_2O	Ignition loss
Gypsum	38.15	3.18	0.32	44.86	1.73	2.57	0.08	8.38

Table 4: Testing instruments for composite cementing material.

Instrument	Supplier
NJ-160A cement paste mixer	Cangzhou Luda Building Instrument Factory
Cement Vicat apparatus	Cangzhou Jilu Testing Instrument Co., Ltd.
SC-145 cement consistometer	Cangzhou Jilu Testing Instrument Co., Ltd.
GZ-85 cement mortar shaking table	Wuxi Jianyi Laboratory Equipment Co., Ltd.
JJ-5 cement mortar mixer	Wuxi Jianyi Laboratory Equipment Co., Ltd.
$70.7 \times 70.7 \times 70.7\ mm^3$ triplex testing mold	Cangzhou Jilu Testing Instrument Co., Ltd.
YH-40B thermostatic and constant humidity box	Hebei Kexi Instruments and Equipment Co., Ltd.
YAW-400 pressure tester	Jinan Haiweier Instrument Co., Ltd.
CP2202S electronic balance	Shenzhen Mingke Chemicals Co., Ltd.
Beakers and measuring cylinders	Shenzhen Ruixinda Scientific and Educational Instruments Co., Ltd.

Table 5: Formulations of composite cementing material.

Test number	Proportioning (%)		
	Portland cement	Sulphoaluminate cement	Gypsum
D01	94.9	3.7	1.4
D02	91.2	3.8	5.0
D03	88.6	1.7	9.7
D04	86.6	11.9	1.5
D05	84.8	9.0	6.2
D06	83.2	5.2	11.6
D07	81.7	0.4	17.9
D08	80.3	14.9	4.8
D09	79.1	9.8	11.1
D10	77.9	4.0	18.1
D11	75.6	15.3	9.1
D12	74.6	8.6	16.8
D13	71.7	14.1	14.2
D14	68.3	11.8	19.9
D15	65.9	18.1	16.0

H_2BO_3) and setting retarding and early strengthening agents (e.g., Li_2CO_3, Na_2SO_4, and $NaNO_2$).

In accordance with Section 2.1, the paste samples were $70.7 \times 70.7 \times 70.7\ mm^3$ cubes and were cured under standard conditions. The setting time and compressive strengths of the samples were measured according to GB1346-89 and GB177-85, respectively.

2.3. Hydration Mechanism of Modified Composite Cementing Material. After being mixed with water, the materials are exposed to a series of physical and chemical reactions and then a hardened body with certain strengths was obtained as cementing pastes which gradually lose fluidity. This process is defined as hydration hardening of cementing material

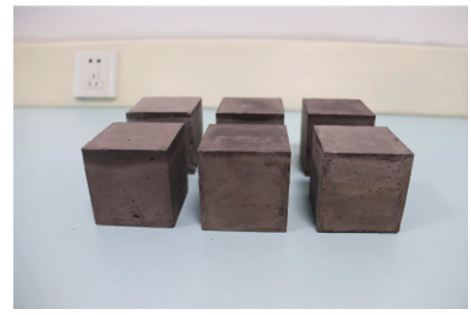

Figure 1: Some of the samples.

[55–64]. The mechanical performances of the hardened body are closely related to hydration products and microstructures of the samples, which vary during the hydration process. Therefore, studies of hydration hardening of cementing material can be conducted in terms of hydration

products and microstructures. Herein, the D09 composite cementing material was selected and made into paste samples according to standard consistency. The samples were cured in a standard curing box for 8 h, 16 h, 1 d, 3 d, and 7 d, respectively. Subsequently, the hydration products and microstructures of prepared paste samples at designated ages were analyzed.

2.3.1. Characterizations by X-Ray Diffraction (XRD). The X′ Pert Pro MPD diffractometer (by Malvern Panalytical, see Figure 2) was employed for quantitative and qualitative analysis of hydration products of the modified composite cementing material. The conditions are as follows: Cu target, Kα diffraction, and scanning angle of 5°~75°. For investigations by XRD, the surface carbonized layers of samples at designated ages were removed and the samples were rinsed twice by acetone and alcohol in CO_2 free environment to achieve complete dehydration. Then, the samples were grinded by using an agate mortar, dried, and sieved by using a 4900 mesh/cm^2 sieve. After each cycle, the mortar was rinsed with HCl.

2.3.2. Characterization by SEM. The microstructures of hydration products were investigated using Apreo high-resolution SEM (see Figure 3). Sample blocks at different ages were dried at 70°C for 2 h, sprayed with gold in vacuum, and then characterized to investigate hydration products and micromorphologies.

3. Results and Discussion

3.1. Compressive Strength and Setting Time of Composite Cementing Materials

3.1.1. Compressive Strength. Table 6 summarizes the setting time and compressive strengths of Portland cement and composite cementing samples measured experimentally at different ages.

As the hydration rate and duration of composites are directly related to chemical compositions of the raw materials, the couplings of the hardened body produced by hydrations inevitably affect the compressive strength of the composite samples. According to the results, the compressive strengths of samples are dependent on the contents of sulphoaluminate cement and gypsum. Figure 4 shows the trends of compressive strengths as a function of composition of composite samples.

As shown in Table 6 and Figure 4, both the early and late compressive strengths of composite cementing material decreased significantly once the content of sulphoaluminate cement exceeded 14% or the content of gypsum exceeded 16%. Indeed, the compressive strengths of composite cementing material may shrink after 3 d in this case. With the content of sulphoaluminate cement below 14% and content of gypsum below 16%, the compressive strengths of composites increased, especially the early strength. The descending sequence of compressive strength is D09 > D06 > D05 > D04 > D02 > D01 > D03. Specifically, compared with Portland cement, compressive strengths of sample D09 at 8 h, 16 h, 1 d, 3 d, 7 d, and 28 d increased by 75%, 42%, 36%, 34%, 24%, and 23%, respectively; meanwhile, compressive

Figure 2: X′ Pert Pro MPD diffractometer.

Figure 3: Apreo high-resolution SEM.

Table 6: Setting time and compressive strengths of samples at different ages.

Test number	Setting time (min)		Compressive strength (MPa)					
	Initial	Final	8 h	16 h	1 d	3 d	7 d	28 d
Portland cement	145	265	2.4	12.8	21.5	29.7	35.8	42.5
D01	22	29	2.9	16.4	25.4	32.7	37.4	44.8
D02	18	25	2.8	18.0	24.6	34.5	39.6	46.3
D03	87	135	2.6	14.8	23.8	30.2	37.6	43.6
D04	8	13	3.2	15.4	28.3	36.4	40.8	47.3
D05	12	20	3.8	17.8	26.4	40.1	43.7	48.9
D06	70	124	3.6	17.4	28.4	38.9	43.8	50.1
D07	187	304	0.6	3.2	5.4	23.2	20.7	18.2
D08	4	8	3.6	13.4	19.3	24.7	18.3	17.2
D09	42	64	4.2	18.2	29.3	39.7	44.5	52.7
D10	85	102	1.4	7.0	12.4	24.1	23.1	21.3
D11	10	13	5.4	10.3	13.2	24.3	20.2	18.9
D12	57	68	2.1	7.9	10.5	14.2	12.1	11.7
D13	12	15	2.7	9.2	14.1	21.3	20.7	19.2
D14	38	52	3.7	6.8	8.7	19.3	18.7	17.1
D15	17	22	3.1	7.2	7.9	18.4	17.2	16.9

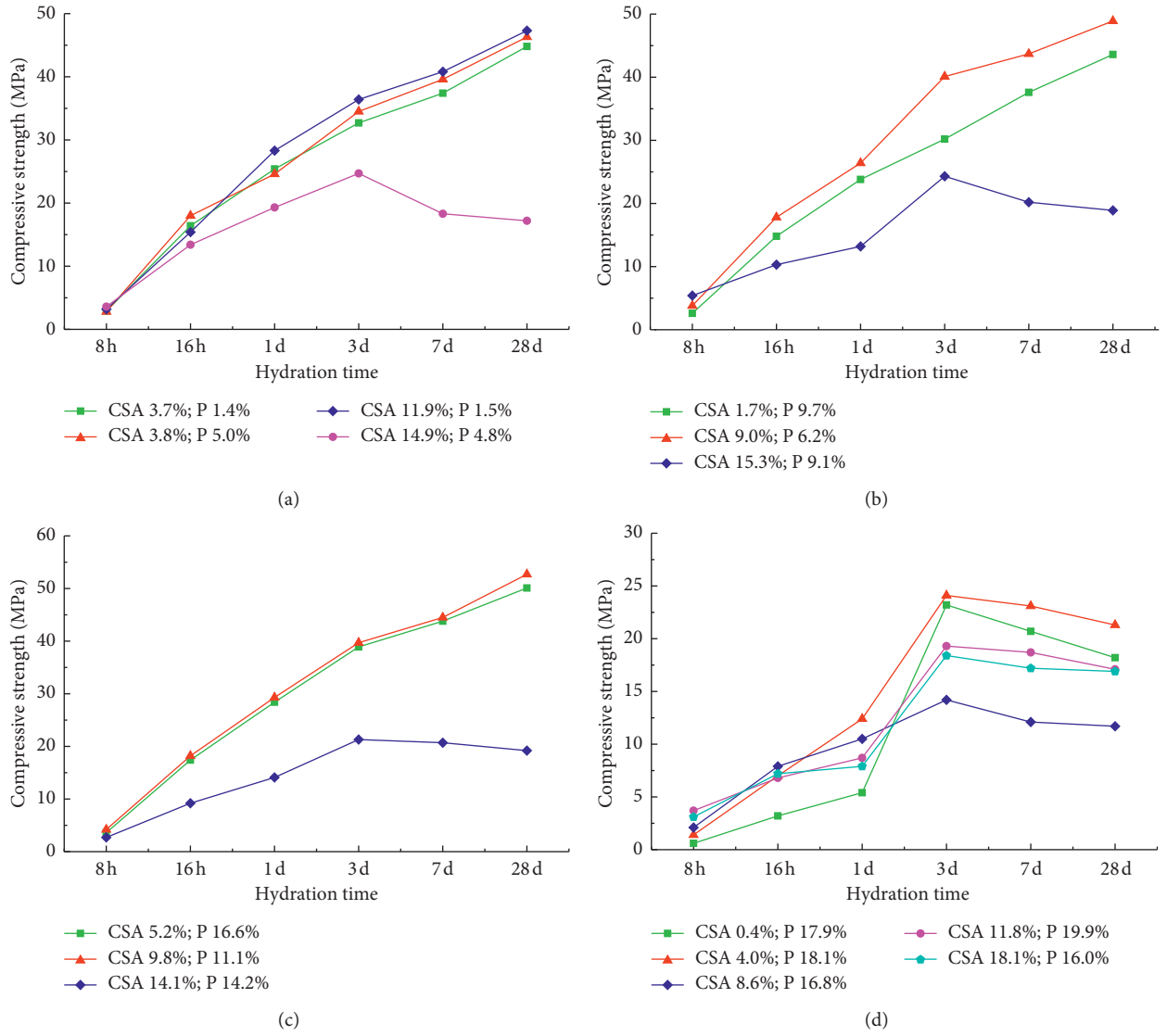

Figure 4: Trends of compressive strengths as a function of sample composition when the gypsum content is (a) 0–5%, (b) 5–10%, (c) 10–15%, and (d) 15–20%. CSA-sulphoaluminate cement; P-gypsum.

strengths of sample D06 at 8 h, 16 h, 1 d, 3 d, 7 d, and 28 d increased by 50%, 36%, 32%, 31%, 22%, and 17%, respectively.

In summary, the early strength of composite cementing samples can be significantly enhanced by ratio optimization of Portland cement, sulphoaluminate cement, and gypsum, as well as the late strength. In terms of structures, hardened bodies by early and late hydration were coupled with each other so that composites exhibited performances superior to the Portland cement single clinker. With compressive strength as the indicator, sample D09 is regarded as the optimized sample in this study.

3.1.2. Setting Time. Figures 5 and 6, respectively, show the initial and final setting time of samples measured experimentally. As observed, the trends of initial and final setting time were consistent: increased as the content of gypsum increased and decreased as the content of sulphoaluminate cement increased. This can be attributed to sulphoaluminate, which accelerates early hydration of the composite samples. As a result, the hydration rate of samples at the early stage increased and the large quantity of hydration products led to reduced setting time. On the other hand, the too high content of gypsum hinders hydration of the Portland cement, resulting in extended setting time of samples.

In summary, despite its significantly enhanced compressive strength, sample D09 exhibited severely reduced initial and final setting time. Indeed, its initial and final setting time was 42 min and 64 min, respectively. The paste filling materials used for mining shall not solidify in channels for 3-4 h. Therefore, the setting time of composite sample D09 optimized by uniform design still does not meet the requirement; thus, modifications by additives are required.

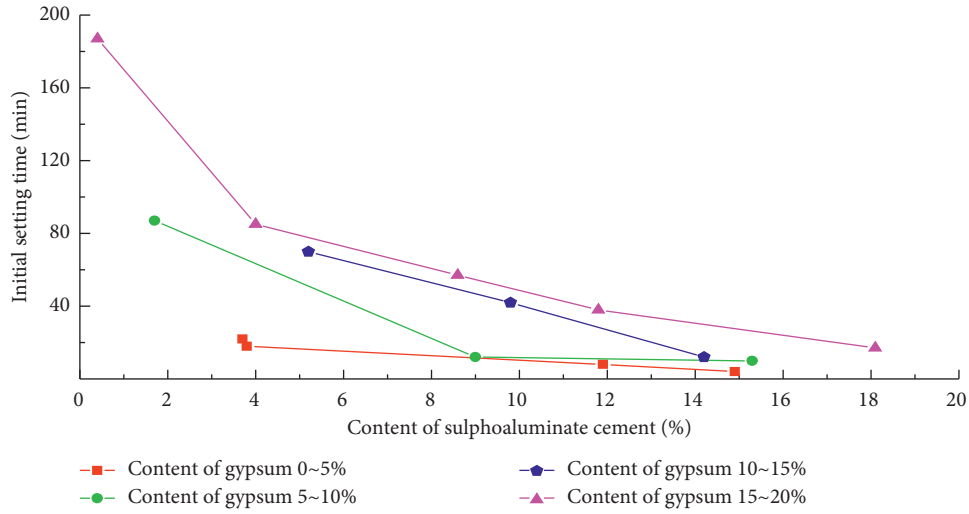

Figure 5: Relationship between initial setting time and components of composite cementing material.

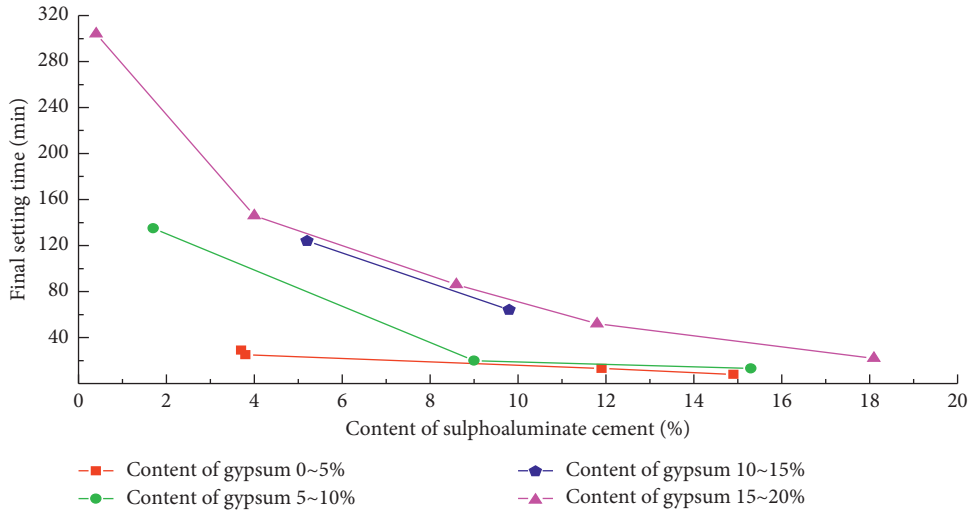

Figure 6: Relationship between final setting time and components of composite cementing material.

3.2. Modification Results of Optimized Composite Cementing Material. Table 7 summarizes the experimentally obtained effects of the setting retarding agent (H_2BO_3) and early strengthening agents (e.g., Li_2CO_3, Na_2SO_4, and $NaNO_2$) on performances of composite cementing material D09.

As observed, Li_2CO_3 and H_2BO_3 had significant effects on the setting time of composite cementing material. As the content of Li_2CO_3 increased, the initial and final setting time decreased and the early strength was enhanced, while the late strength decreased. As the content of H_2BO_3 increased, the initial and final setting time increased, while the early strength decreased. The results indicated that at the expense of reduced late strengths, additive J6 had desired effects on the setting time and early strength, while additives J7 and J8 can enhance both setting time and compressive strengths. Therefore, H_2BO_3 (0.3%) + Na_2SO_4 (0.1%) and H_2BO_3 (0.3%) + $NaNO_2$ (0.1%) are ideal setting retarding and early strengthening additives for composite cementing material.

In summary, appropriate additives can enhance the performances (e.g., setting time and compressive strengths) of composite cementing material. In this study, samples J7 and J8 are ideal additives for cementing material in coal mining filling.

3.3. Hydration Mechanism of Modified Composite Cementing Material

3.3.1. Hydration Process. The composite cementing material consists of $2CaO{\cdot}SiO_2$, $3CaO{\cdot}SiO_2$, $3CaO{\cdot}Al_2O_3$, $4CaO{\cdot}Al_2O_3{\cdot}Fe_2O_3$ (Portland cement), $3CaO{\cdot}3Al_2O_3{\cdot}CaSO_4$, $2CaO{\cdot}SiO_2$ (sulphoaluminate cement), and $CaSO_4{\cdot}2H_2O$ (gypsum). Owing to the presence of gypsum, the reaction rate of $3CaO{\cdot}Al_2O_3$ and $3CaO{\cdot}SiO_2$ was higher than that of $2CaO{\cdot}SiO_2$ and $4CaO{\cdot}Al_2O_3{\cdot}Fe_2O_3$. Meanwhile, $3CaO{\cdot}3Al_2O_3{\cdot}CaSO_4$ in sulphoaluminate is an early hydration

Table 7: Effects of additives on performances of composite cementing material.

Test number	Contents of additives (%)	Setting time (min)		Compressive strength (MPa)					
		Initial	Final	8 h	16 h	1 d	3 d	7 d	28 d
J1	D09	42	64	4.2	18.2	29.3	39.7	44.5	52.7
J2	Li_2CO_3 (0.15)	21	32	6.1	23.5	26.7	30.2	34.4	40.5
J3	Li_2CO_3 (0.30)	18	27	8.4	25.4	24.1	27.6	32.7	38.4
J4	H_2BO_3 (0.15)	125	184	2.0	12.7	20.7	34.2	39.5	51.2
J5	H_2BO_3 (0.3)	324	348	1.2	10.4	18.6	32.1	38.8	50.7
J6	H_2BO_3 (0.3) + Li_2CO_3 (0.1)	152	182	5.8	24.6	28.7	32.2	36.4	39.3
J7	H_2BO_3 (0.3) + Na_2SO_4 (0.1)	182	185	5.8	22.8	34.2	46.5	49.7	58.4
J8	H_2BO_3 (0.3) + $NaNO_2$ (0.1)	214	232	5.2	19.5	32.9	43.2	47.3	54.1

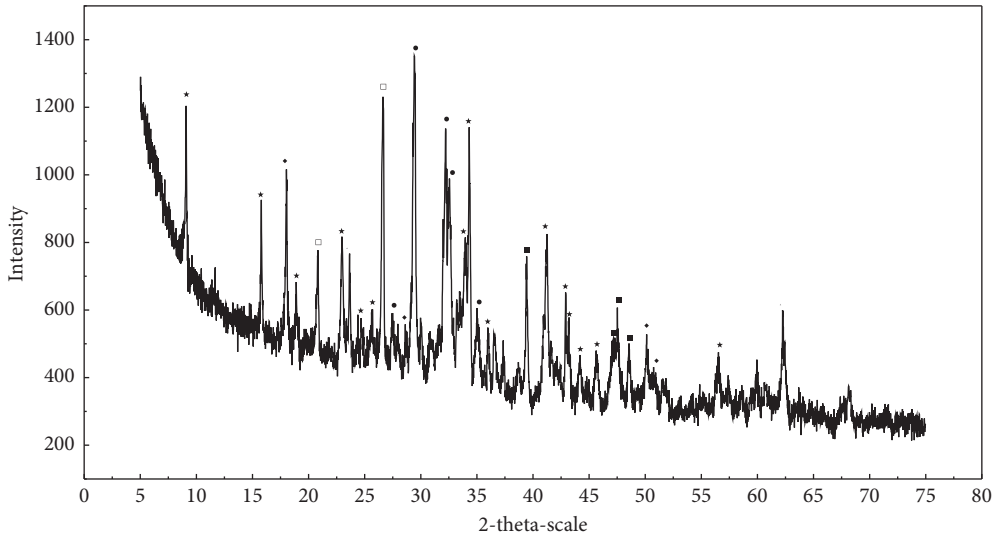

(a)

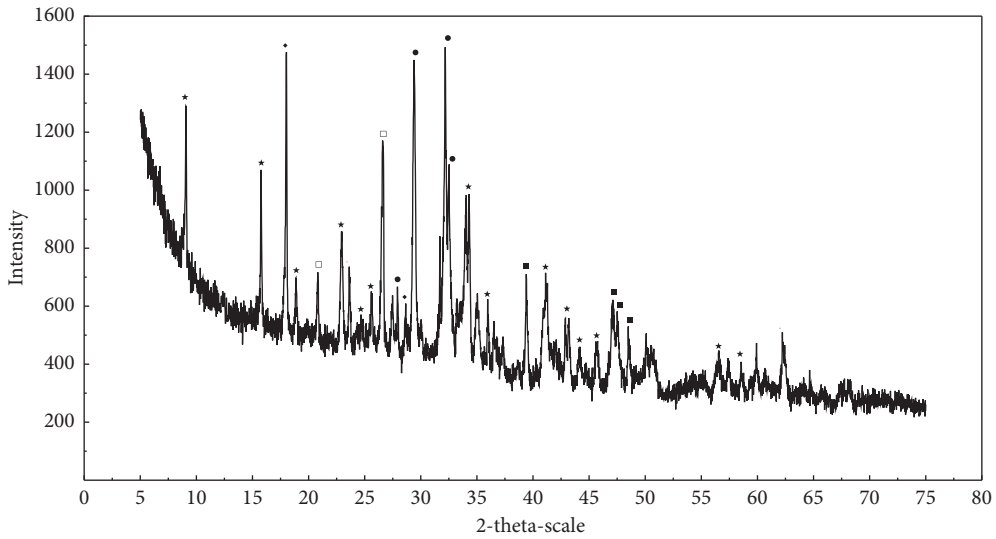

(b)

Figure 7: Continued.

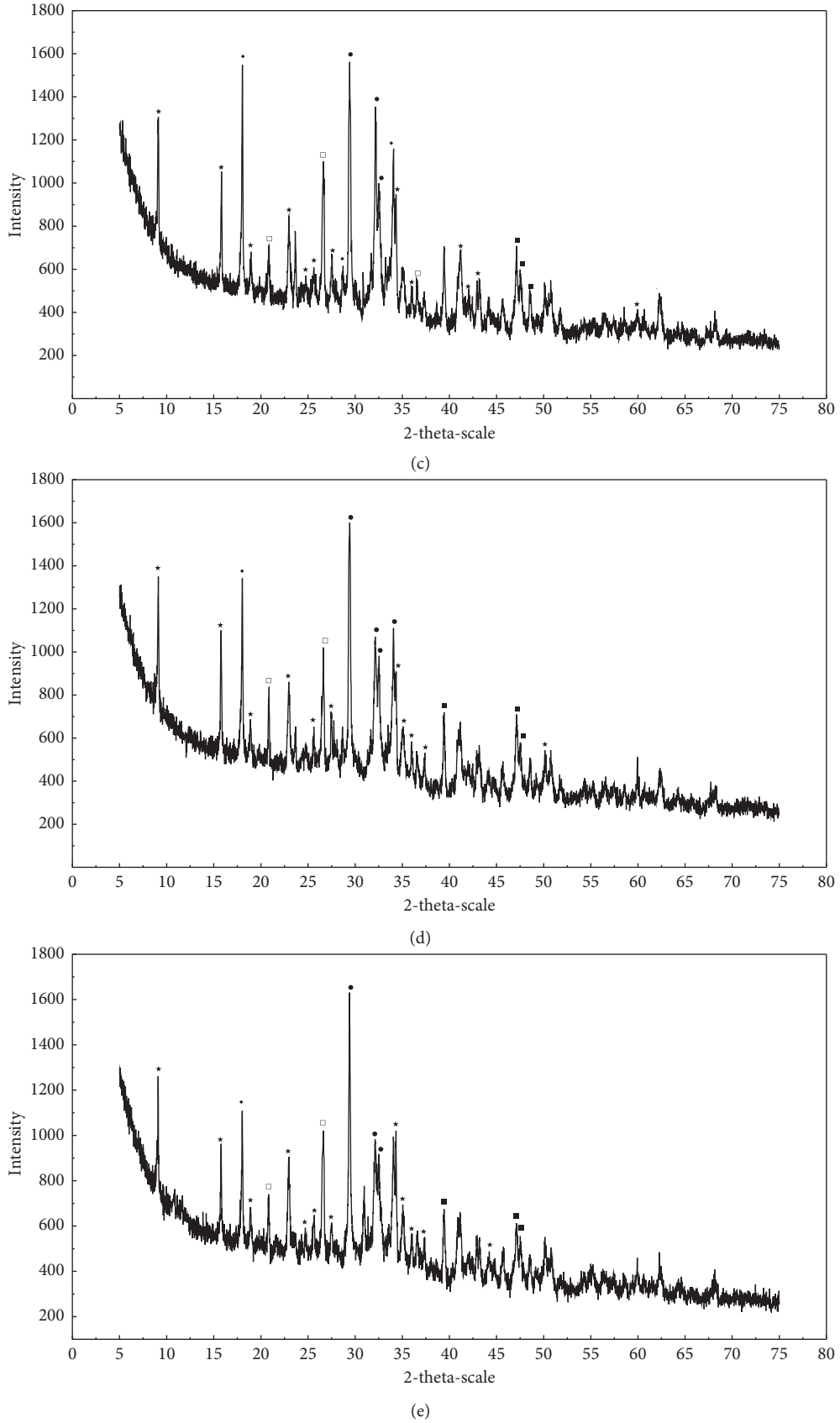

Figure 7: XRD spectra of samples at different hydration ages. ★-AFt; ◁-C-S-H; ◆-CH; ■-$CaCO_3$; □-SiO_2; △-$3CaO{\cdot}3Al_2O_3{\cdot}CaSO_4$. (a) 8 h. (b) 16 h. (c) 1 d. (d) 3 d. (e) 7 d.

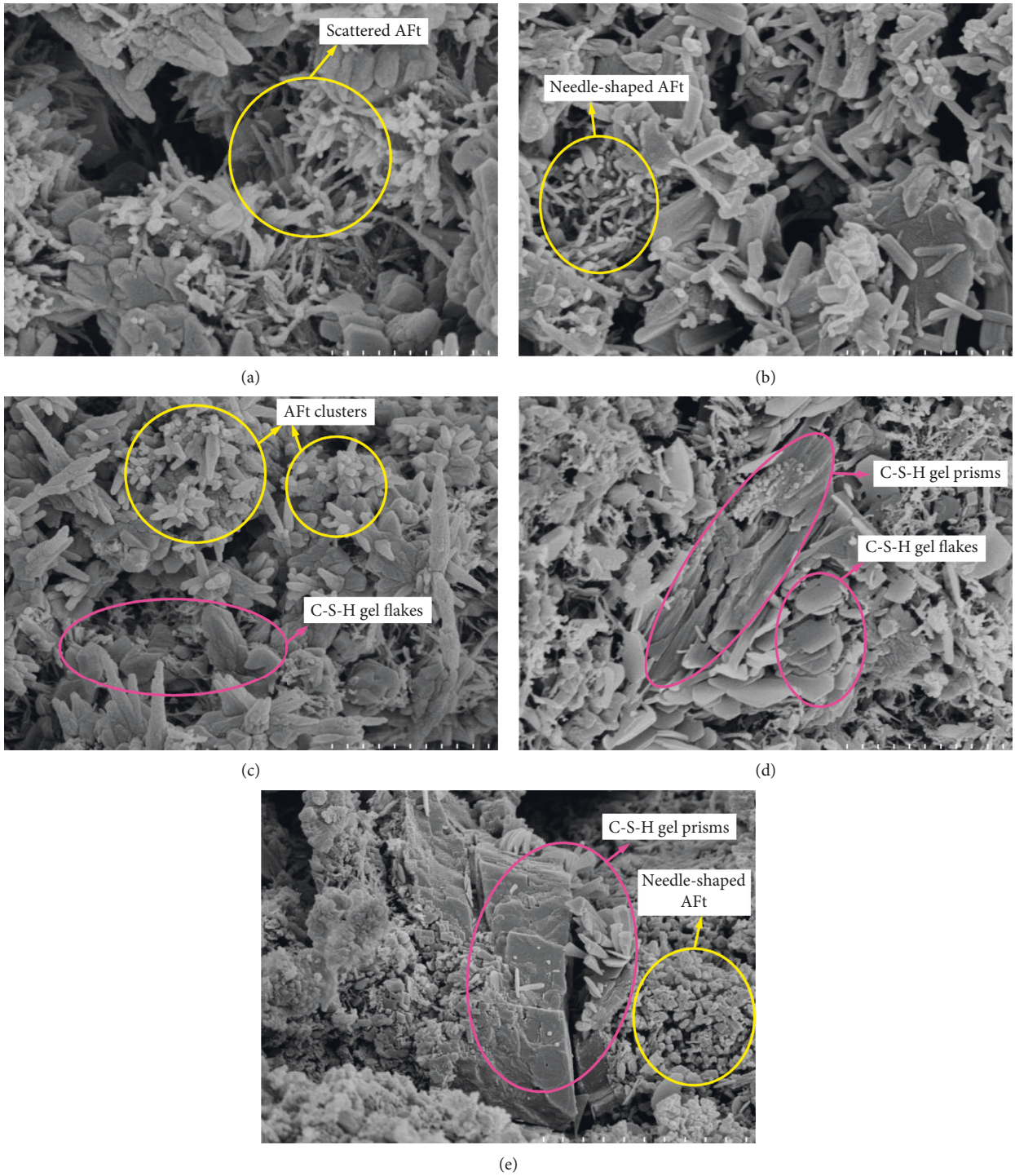

Figure 8: SEM images of samples at different ages. (a) 8 h. (b) 16 h. (c) 1 d. (d) 3 d. (e) 7 d.

product. Therefore, $3CaO{\cdot}3Al_2O_3{\cdot}CaSO_4$, $3CaO{\cdot}Al_2O_3$, and $3CaO{\cdot}SiO_2$ react with each other upon addition of water:

$$3CaO{\cdot}3Al_2O_3{\cdot}CaSO_4 + 38H_2O = 3CaO{\cdot}Al_2O_3{\cdot}CaSO_4{\cdot}32H_2O + 2(Al_2O_3{\cdot}H_2O)$$

$$3CaO{\cdot}Al_2O_3 + 3CaSO_4{\cdot}2H_2O + 26H_2O = 3CaO{\cdot}Al_2O_3{\cdot}3CaSO_4{\cdot}32H_2O$$

$$2(3CaO{\cdot}SiO_2) + 11H_2O = 3CaO{\cdot}2SiO_2{\cdot}8H_2O + 3Ca(OH)_2$$

As the hydration proceeds, the concentration of $Ca(OH)_2$ increases and hydration products react with gypsum:

$$Al_2O_3{\cdot}H_2O + 3Ca(OH)_2 + 3CaSO_4{\cdot}2H_2O + 22H_2O = 3CaO{\cdot}Al_2O_3{\cdot}3CaSO_4{\cdot}32H_2O$$

In the middle and late hydration stages, $2CaO{\cdot}SiO_2$ and $4CaO{\cdot}Al_2O_3{\cdot}Fe_2O_3$ are activated:

$$2(2CaO{\cdot}SiO_2) + 9H_2O = 3CaO{\cdot}2SiO_2{\cdot}8H_2O + Ca(OH)_2$$

$$C_4AF + 2CH + 6CaSO_4{\cdot}2H_2O + 50H = 2C_3(A, F){\cdot}3CaSO_4{\cdot}32H_2O$$

In summary, main hydration products of the samples include ettringite (AFt), calcium hydroxide (CH) gel, and hydrated calcium silicate (C-S-H) gel. The generation of AFt at an early stage is the main cause of high early strength of samples.

3.3.2. Hydration Products. Figure 7 shows the XRD spectra of samples at different hydration ages. Several conclusions can be drawn:

(1) The main hydration products include AFt, CH gel, and C-S-H gel, while their relative contents vary with the hydration age, according to their diffraction peak intensities

(2) After 8 h hydration, a considerable quantity of AFt was generated, resulting in high early strength of samples

(3) $CaCO_3$ was observed in hydration products. This can be attributed to the exposure of AFt to CO_2

(4) The diffraction peaks of clinker minerals (e.g., SiO_2 and $3CaO{\cdot}3Al_2O_3{\cdot}CaSO_4$) in samples decreased, indicating that the contents of clinker minerals decreased as the hydration age increased

(5) After 8 h of hydration, no diffraction peak corresponding to $CaSO_4$ was observed, demonstrating complete hydration of $CaSO_4$, whose product is AFt

3.3.3. Microstructures. Figure 8 shows the microstructures of samples at different hydration ages. Several conclusions can be drawn:

(1) After 8 h of hydration, fine, scattered, needle-shaped AFt was observed. The AFt grew interactively and radially, with high density.

(2) After 16 h, the density of AFt increased, and its growth followed the intersecting pattern.

(3) After 1 d of hydration, sizes of AFt increased drastically and were distributed in clusters, while C-S-H gel flakes appeared.

(4) After 3 d, the density of C-S-H gel increased and the flakes were turned into prisms, demonstrating that the contents of C-S-H gel and CH gel increased and the hydration of Portland cement was accelerated.

(5) After 7 d, the matrix AFt followed a cloud distribution while the density of needle-shaped AFt decreased. In some areas, large C-S-H gel prisms were observed.

(6) According to the microstructures of hydration products, the early and late strength of sample was dominated by AFt and C-S-H gel, respectively, as AFt grew rapidly while C-S-H gel grew slowly. The hydration products grew interactively and were coupled, thus facilitating the growth of the hardened bodies of cementing material, instead of restraining each other due to the generation sequence.

4. Conclusions

Formulation tests of composite cementing materials were conducted based on constrained formulation design. The effects of compositions (e.g., Portland cement, sulphoaluminate cement, and gypsum) of composite cementing materials on their performances were investigated using mechanical performance tests of samples, and the optimized samples were tested and modified. The following conclusions can be drawn:

(1) The setting time of samples was negatively related to the content of sulphoaluminate cement and positively related to the content of gypsum, and the trends of initial and final setting time were consistent.

(2) Both the early and late compressive strengths of composite cementing materials decreased significantly if the content of sulphoaluminate cement exceeded 14% or the content of gypsum exceeded 16%. Indeed, the compressive strengths of composite cementing material may shrink after 3 d in this case. With the content of sulphoaluminate cement below 14% and the content of gypsum below 16%, the compressive strengths of composites increased. The composition corresponding to optimized compressive strength was Portland cement (79.1%) + sulphoaluminate cement (9.8%) + hardened gypsum (11.1%).

(3) Additives $H_2BO_3(0.3\%) + Na_2SO_4(0.1\%)$ and $H_2BO_3(0.3\%) + NaNO_2(0.1\%)$ are regarded as setting retarding and early strengthening composite additives because they can enhance both the setting time and the strength of composite cementing material.

(4) Investigations by XRD and SEM revealed that the hydration products were dominated by AFt at the early stage and C-S-H gel and CH gel at the middle and late stages. Meanwhile, hydration products of composite cementing material with optimized ratios grew interactively and were coupled, thus facilitating the growth of the hardened body of cementing material, instead of restraining each other due to the generation sequence.

In this study, the optimized ratios of Portland cement, sulphoaluminate cement, and gypsum in composite cementing material were determined, the hydration mechanism of composite cementing material was identified, and the composite cementing material was modified using appropriate additives to meet the requirements by paste filling in coal mines.

Appendix

Over the past two decades, uniform design has been widely applied, especially in formulation design for materials. Known as mixing tests, formulation tests aim to investigate

the effects of material ratio on performance indicators. The formulation design can be categorized as unconstrained and constrained ones according to component constraints in the formulation.

In composite cementing material, the contents of sulphoaluminate cement and gypsum were relatively low as they are employed to modify the properties of Portland cement. Hence, samples in this study shall be tested by constrained formulation tests with s kinds of raw materials $M_1, M_2, \ldots, M_s$ and with percentage contents of $X_1, X_2, \ldots, X_s$, respectively; optimized formulation was researched under constraints:

(1) Define the constraints of $X_1, X_2, \ldots, X_s$ in the formulation as

$$\begin{cases} X_1 + X_2 + \wedge + X_s = 1, \\ a_i \le X_i \le b_i, \quad i = 1, \wedge, s. \end{cases} \tag{A.1}$$

(2) With given s and n, appropriate uniform design table was selected accordingly and the set of elements in $U_n^*(n^{s-1})$ or $U_n(n^{s-1})$ was labelled as $\{q_{ki}\}$.

(3) The selected uniform design table $U_n^*(n^{s-1})$ or $U_n(n^{s-1})$ was linearly transformed to a unit cube vector c_{ki}:

$$c_{ki} = \frac{2q_{ki} - 1}{2n}, \quad i = 1, \wedge, s-1, \; k = 1, \wedge, n. \tag{A.2}$$

(4) Define $\{(c_{k1}, c_{k2}, \wedge, c_{ks}), k = 1, \wedge, n\}$ as a group of uniformly distributed points in C^s and calculate $\{x_{ki}\}$ using equation (A.3) and obtain equation (A.4) based on constraints of x_{ki}:

$$\begin{cases} x_{ki} = \left(1 - c_{ki}^{1/s-i}\right) \prod_{j=1}^{i-1} c_{kj}^{1/s-j}, & i = 1, \wedge, s-1, \\ x_{ks} = \prod_{j=1}^{s-1} c_{kj}^{1/s-j}, & k = 1, \wedge, n, \end{cases} \tag{A.3}$$

$$\begin{cases} a_i < x_{ki} < b_i, & i = 1, \wedge, s-1 \\ a_s < x_{ks} < b_s, & k = 1, \wedge, n. \end{cases} \tag{A.4}$$

Solve that to obtain $c_{ki}^{\min}$ and $c_{ki}^{\max}$, which are minimum and maximum of c_{ki}, respectively. In this way, simplex T_s was obtained and the area determined by I_s is defined as R:

$$R = \left\{ \left[c_{k1}^{\min}, c_{k1}^{\max}\right] \times \left[c_{k2}^{\min}, c_{k2}^{\max}\right] \times \wedge \times \left[c_{ks}^{\min}, c_{ks}^{\max}\right] \right\}. \tag{A.5}$$

Set a uniform design in R and define the area confined by $\{c_{ki}\}$ as area D. Then, points in D are the uniform design scheme needed for this study.

(5) Points in $\{c_{ki}\}$ are linearly transformed to R to generate $\{c_{ki}^*\}$:

$$c_{ki}^* = c_{ki}^{\min} + \left(c_{ki}^{\max} - c_{ki}^{\min}\right) \times c_{ki}, \quad i = 1, \wedge, s, \; k = 1, \wedge, n. \tag{A.6}$$

(6) Points in $\{c_{ki}^*\}$ that follow equations (A.3) and (A.4) are included in area D.

(7) Substitute points in area D into equation (A.3) to obtain $\{x_{ki}\}$.

Data Availability

All data used to support the findings of this study are available from the corresponding author upon request.

Additional Points

Highlights. (1) Providing references for further enhancing the performances of composite cementing material for paste filling in coal mines. (2) Effects of the contents of sulphoaluminate cement and gypsum on composite cementing material' setting time and compressive strength are investigated. (3) Two kinds of optimized additives, which are (H_2BO_3 (0.3%) + Na_2SO_4 (0.1%) and H_2BO_3 (0.3%) + $NaNO_2$ (0.1%)), have been identified to enhance setting time and strength of composite cementing material for paste filling in coal mines.

Conflicts of Interest

The authors declare that they have no conflicts of interest.

Acknowledgments

This work was supported by the Key Laboratory of Deep Coal Mine Excavation Response and Disaster Prevention and Control, Anhui Province (Anhui University of Science and Technology), Huainan, China, 232001, (KLDCMERDPC16101 and 01CK05002), Jinxiao Liu (liujinxiao1999@126.com) and the Key Development Plan Financial Aid Project of Shandong, China, (2018GSF116002), Xinguo Zhang (Zhangxg@sdust.edu.cn), and the National Science Fund Financial Aid Project, (51574159), Xinguo Zhang (Zhangxg@sdust.edu.cn).

References

[1] B. Yang and J. Yang, "Development and selection on filling technology of coal mine," *Industrial Minerals & Processing*, vol. 35, no. 5, pp. 11–15, 2015.

[2] X. Miao, F. Ju, Y. Huang, and G. Guo, "New development and prospect of backfilling mining theory and technology," *Journal of China University of Mining & Technology*, vol. 44, no. 3, pp. 391–399, 2015.

[3] B. Hu, "Backfill mining technology and development tendency in China coal mine," *Coal Science and Technology*, vol. 40, no. 11, pp. 1–5, 2012.

[4] B. S. Choudhary and S. Kumar, "Underground void filling by cemented mill tailings," *International Journal of Mining Science and Technology*, vol. 23, no. 6, pp. 893–900, 2013.

[5] A. Ghirian and M. Fall, "Strength evolution and deformation behaviour of cemented paste backfill at early ages: effect of curing stress, filling strategy and drainage," *International Journal of Mining Science and Technology*, vol. 26, no. 5, pp. 809–817, 2016.

[6] D. Ouattara, A. Yahia, M. Mbonimpa, and T. Belem, "Effects of superplasticizer on rheological properties of cemented paste backfills," *International Journal of Mineral Processing*, vol. 161, no. 10, pp. 28–40, 2017.

[7] S. Yang, S. Su, and F. Wang, "Analysis of strength regularity of high concentration tailings cemented backfill," *Bulletin of the Chinese Ceramic Society*, vol. 38, no. 3, pp. 847–852, 2019.

[8] S. Yang and Y. Fu, "Tudy on evolution of damage on postpeak bearing stage of tailings filling body by cement-sand ratio," *Industrial Minerals & Processing*, vol. 47, no. 4, pp. 26–28, 2018.

[9] L. Jian and F. Deng, "Experimental study on long-term strength of full tailings cemented backfill," *Industrial Minerals & Processing*, vol. 47, no. 10, pp. 47–49, 2018.

[10] W. Liu, Y. Rao, W. Xu, X. Hong, Z. Liu, and M. Han, "Effect of acidic corrosion on physical and mechanical properties of full tailings cemented backfill," *Mining Research and Development*, vol. 38, no. 3, pp. 91–94, 2018.

[11] W. Yang, Q. Zhang, S. Yang, and X. Wang, "Mechanical property of high concentration total tailing cemented backfilling under dynamic loading," *Journal of Central South University (Science and Technology)*, vol. 48, no. 1, pp. 156–161, 2017.

[12] B. Yang, *Numerical Simulation and Application Research of High Concentration of Cemented Full Tailing Backfilling Pipeline Transportation*, University of South China, Hengyang, China, 2016.

[13] H. Wang, "The characterization of activated calcium carbonate with the rate of suspension in water," *Industrial Minerals & Processing*, vol. 12, no. 12, pp. 16–18, 2000.

[14] H. He, T. Huang, and Y. Xu, "An experimental study on technology of cemented filling with high-water quick consolidating tailings and its operation in fankou lead-zinc mine," *Mining Research and Development*, vol. 16, no. S1, pp. 16–20, 1996.

[15] G. Ding and C. Li, "Experiment on high-water quick consolidated filling with single piping unclassified tailings in fenghuangshan copper mine," *Mining Research and Development*, vol. 16, no. S1, pp. 90–92, 1996.

[16] G. He, Y. Liu, D. Ding, and Z. Zhang, "Strength characteristic of cemented waste rock backfills and its application," *Journal of Mining & Safety Engineering*, vol. 30, no. S1, pp. 74–79, 2013.

[17] S. Lu and X. Wang, "Study on the influence of rock block proportion and shape on the mechanical properties of cemented filling body," *Mining Research and Development*, vol. 38, no. 3, pp. 73–76, 2018.

[18] H. Ren, H. Wang, and M. Li, "Technical study on stripty peand pre-supportmining method with subsequent cemented rock fill," *Industrial Minerals & Processing*, vol. 46, no. 12, pp. 64–67, 2017.

[19] F. Xiao, Y. Zhuo, C. Chen, J. Han, X. Wang, and Y. Hu, "Study on mechanical properties and acoustic emission characteristics of cemented filling body," *Industrial Minerals & Processing*, vol. 45, no. 9, pp. 44–47, 2016.

[20] F. Xiao, S. Cao, Y. Zhuo, Y. Li, J. Han, and X. Wang, "Destructive tests on the cemented rock filling body under different stress paths," *Mining Research and Development*, vol. 36, no. 7, pp. 43–46, 2016.

[21] X. Wang, Y. Zhuo, C. Chen, J. Han, F. Xiao, and Y. Hu, "Study on the main harmful material under failure process of blocky rock cemented filling body," *Mining Research and Development*, vol. 36, no. 2, pp. 43–47, 2016.

[22] L. Zhang, A. Wu, and H. Wang, "Effects and mechanism of pumping agent on rheological properties of highly muddy paste," *Chinese Journal of Engineering*, vol. 40, no. 8, pp. 918–924, 2018.

[23] J. Zhang, K. Wang, X. Zhang, J. Yan, and Y. Zheng, "Analysis on creep characteristics of paste filling materials in residual roadway support," *Mining Research and Development*, vol. 38, no. 3, pp. 95–99, 2018.

[24] J. Liu, J. Li, and G. Wang, "Simulation study on the paste pumping system with dual-pump parallel based on AMESim," *Mining Research and Development*, vol. 37, no. 11, pp. 86–89, 2017.

[25] C. Chen and S. Cai, "Issues related to the pilot operation of paste filling system in Jingchuan's no. 2 mining district," *Mining Research and Development*, vol. 21, no. 3, pp. 21–23, 2001.

[26] T. Qi and G. Feng, "Resistivity and AE Response characteristics in the failure process of CGB under uniaxial loading," *Advances in Materials Science and Engineering*, vol. 2017, Article ID 7857590, 11 pages, 2017.

[27] T. Qi, G. Feng, Y. Li, Y. Guo, J. Guo, and Y. Zhang, "Effects of fine gangue on strength, resistivity, and microscopic properties of cemented coal gangue backfill for coal mining," *Shock and Vibration*, vol. 2015, Article ID 752678, 11 pages, 2015.

[28] Q. Li, G. Feng, Y. Guo et al., "The dosage of superplasticizer in cemented coal waste backfill material based on Response surface methodology," *Advances in Materials Science and Engineering*, vol. 2019, Article ID 5328523, 2019.

[29] M. Fall and M. Benzaazoua, "Modeling the effect of sulphate on strength development of paste backfill and binder mixture optimization," *Cement and Concrete Research*, vol. 35, no. 2, pp. 301–314, 2005.

[30] M. Fall and M. Pokharel, "Coupled effects of sulphate and temperature on the strength development of cemented tailings backfills: portland cement-paste backfill," *Cement & Concrete Composites*, vol. 32, no. 10, pp. 819–828, 2010.

[31] W. Li and M. Fall, "Strength and self-desiccation of slag-cemented paste backfill at early ages: link to initial sulphate concentration," *Cement and Concrete Composites*, vol. 89, pp. 160–168, 2018.

[32] J. Tailby and K. J. D. MacKenzie, "Structure and mechanical properties of aluminosilicate geopolymer composites with portland cement and its constituent minerals," *Cement and Concrete Research*, vol. 40, no. 5, pp. 787–794, 2010.

[33] M. Saafi, L. Tang, J. Fung, M. Rahman, and J. Liggat, "Enhanced properties of graphene/fly ash geopolymeric composite cement," *Cement and Concrete Research*, vol. 67, pp. 292–299, 2015.

[34] K. Kupwade-Patil, M. Tyagi, C. M. Brown, and O. Büyüköztürk, "Water dynamics in cement paste at early age prepared with pozzolanic volcanic ash and ordinary portland cement using quasielastic neutron scattering," *Cement and Concrete Research*, vol. 86, pp. 55–62, 2016.

[35] B. Feneuil, N. Roussel, and O. Pitois, "Optimal cement paste yield stress for the production of stable cement foams," *Cement and Concrete Research*, vol. 120, pp. 142–151, 2019.

[36] A. Kesimal, B. Ercikdi, and E. Yilmaz, "The effect of desliming by sedimentation on paste backfill performance," *Minerals Engineering*, vol. 16, no. 10, pp. 1009–1011, 2003.

[37] A. Arora, G. Sant, and N. Neithalath, "Ternary blends containing slag and interground/blended limestone: hydration, strength, and pore structure," *Construction and Building Materials*, vol. 102, pp. 113–124, 2016.

[38] S. Adu-Amankwah, L. Black, J. Skocek, M. B. Haha, and M. Zajac, "Effect of sulfate additions on hydration and performance of ternary slag-limestone composite cements," *Construction and Building Materials*, vol. 164, pp. 451–462, 2018.

[39] B. Lu, C. Shi, J. Zhang, and J. Wang, "Effects of carbonated hardened cement paste powder on hydration and microstructure of portland cement," *Construction and Building Materials*, vol. 186, pp. 699–708, 2018.

[40] Y.-F. Cao, Z. Tao, Z. Pan, and R. Wuhrer, "Effect of calcium aluminate cement on geopolymer concrete cured at ambient temperature," *Construction and Building Materials*, vol. 191, pp. 242–252, 2018.

[41] E.-J. Moon and Y. C. Choi, "Carbon dioxide fixation via accelerated carbonation of cement-based materials: potential for construction materials applications," *Construction and Building Materials*, vol. 199, pp. 676–687, 2019.

[42] Z. Prošek, V. Nežerka, R. Hlůžek, J. Trejbal, P. Tesárek, and G. Karra'a, "Role of lime, fly ash, and slag in cement pastes containing recycled concrete fines," *Construction and Building Materials*, vol. 201, pp. 702–714, 2019.

[43] T. Shi, Z. Li, J. Guo, H. Gong, and C. Gu, "Research progress on CNTs/CNFs-modified cement-based composites—a review," *Construction and Building Materials*, vol. 202, pp. 290–307, 2019.

[44] S. J. Lee, C. H. Lee, M. Shin, S. Bhattacharya, and Y. F. Su, "Influence of coarse aggregate angularity on the mechanical performance of cement-based materials," *Construction and Building Materials*, vol. 204, pp. 184–192, 2019.

[45] D. Wang, C. Shi, N. Farzadnia et al., "A quantitative study on physical and chemical effects of limestone powder on properties of cement pastes," *Construction and Building Materials*, vol. 204, pp. 58–69, 2019.

[46] B. Sun, H. Wu, W. Song, Z. Li, and J. Yu, "Design methodology and mechanical properties of superabsorbent polymer (SAP) cement-based materials," *Construction and Building Materials*, vol. 204, pp. 440–449, 2019.

[47] A. A. Ramezanianpour, E. Ghiasvand, I. Nickseresht, M. Mahdikhani, and F. Moodi, "Influence of various amounts of limestone powder on performance of portland limestone cement concretes," *Cement and Concrete Composites*, vol. 31, no. 10, pp. 715–720, 2009.

[48] K. De Weerdt, K. O. Kjellsen, E. Sellevold, and H. Justnes, "Synergy between fly ash and limestone powder in ternary cements," *Cement and Concrete Composites*, vol. 33, no. 1, pp. 30–38, 2011.

[49] E. F. Irassar, D. Violin, V. F. Rahhal, C. Milanes, M. A. Trezza, and V. L. Bonavetti, "Influence of limestone content, gypsum content and fineness on early age properties of Portland limestone cement produced by inter-grinding," *Cement and Concrete Composites*, vol. 33, no. 2, pp. 192–200, 2011.

[50] V. Kirk, M. Aguayo, T. Oey, G. Sant, and N. Narayanan, "Hydration and strength development in ternary portland cement blends containing limestone and fly ash or metakaolin," *Cement and Concrete Composites*, vol. 39, pp. 93–103, 2013.

[51] A. Kumar, T. Oey, S. Kim et al., "Simple methods to estimate the influence of limestone fillers on reaction and property evolution in cementitious materials," *Cement and Concrete Composites*, vol. 42, pp. 20–29, 2013.

[52] V. Afroughsabet, G. Geng, A. Lin et al., "The influence of expansive cement on the mechanical, physical, and microstructural properties of hybrid-fiber-reinforced concrete," *Cement and Concrete Composites*, vol. 96, pp. 21–32, 2019.

[53] G. R. Feng, X. Q. Jia, Y. X. Guo et al., "Study on mixture ratio of gangue-waste concrete cemented paste backfill," *Journal of Mining & Safety Engineering*, vol. 33, no. 6, pp. 1072–1079, 2016.

[54] T. Qi, F. Guorui, Y. Guo et al., "Experimental study on the changes of coal paste backfilling material performance during hydration process," *Journal of Mining & Safety Engineering*, vol. 32, no. 1, pp. 42–48, 2015.

[55] A. Ren, G. R. Feng, Y. X. Guo et al., "Influence on performance of coal mine filling paste with fly ash," *Journal of China Coal Society*, vol. 39, no. 12, pp. 2374–2380, 2014.

[56] X. Zhang, H. Wang, Y. Li, and J. Shi, "Experimental research for influencing factors on properties of paste filling materials," *Journal of Shandong University of Science and Technology (Natural Science)*, vol. 31, no. 3, pp. 53–58, 2012.

[57] Z. Cui and H. Sun, "The preparation and properties of coal gangue based sialite paste like back fill material," *Journal of China Coal Society*, vol. 35, no. 6, pp. 896–899, 2010.

[58] V. Shah, K. Scrivener, B. Bhattacharjee, and S. Bishnoi, "Changes in microstructure characteristics of cement paste on carbonation," *Cement and Concrete Research*, vol. 109, pp. 184–197, 2018.

[59] S. Adu-Amankwah, M. Zajac, C. Stabler, B. Lothenbach, and L. Black, "Influence of limestone on the hydration of ternary slag cements," *Cement and Concrete Research*, vol. 100, pp. 96–109, 2017.

[60] F. Hueller, C. Naber, J. Neubauer, and F. Goetz-Neunhoeffer, "Impact of initial CA dissolution on the hydration mechanism of CAC," *Cement and Concrete Research*, vol. 113, pp. 41–54, 2018.

[61] M. Wyrzykowski, K. Scrivener, and P. Lura, "Basic creep of cement paste at early age—the role of cement hydration," *Cement and Concrete Research*, vol. 116, pp. 191–201, 2019.

[62] D. Wang, C. Shi, N. Farzadnia, Z. Shi, H. Jia, and Z. Ou, "A review on use of limestone powder in cement-based materials: mechanism, hydration and microstructures," *Construction and Building Materials*, vol. 181, pp. 659–672, 2018.

[63] X. Yang, E. Kuru, M. Gingras, and S. Iremonger, "CT-CFD integrated investigation into porosity and permeability of neat early-age well cement at downhole condition," *Construction and Building Materials*, vol. 205, pp. 73–86, 2019.

[64] W. Ashraf, "Carbonation of cement-based materials: challenges and opportunities," *Construction and Building Materials*, vol. 120, pp. 558–570, 2016.

[65] F. Li and J. Liu, "An experimental investigation of hydration mechanism of cement with silicane," *Construction and Building Materials*, vol. 166, pp. 684–693, 2018.

[66] X. Wang, K. Xu, Y. Li, and S. Guo, "Dissolution and leaching mechanisms of calcium ions in cement based materials," *Construction and Building Materials*, vol. 180, pp. 103–108, 2018.

[67] Y. Zha, J. Yu, R. Wang, P. He, and Z. Cao, "Effect of ion chelating agent on self-healing performance of cement-based materials," *Construction and Building Materials*, vol. 190, pp. 308–316, 2018.